

Colorimetric and Ratiometric Red Fluorescent Chemosensor for Fluoride Ion Based on Diketopyrrolopyrrole

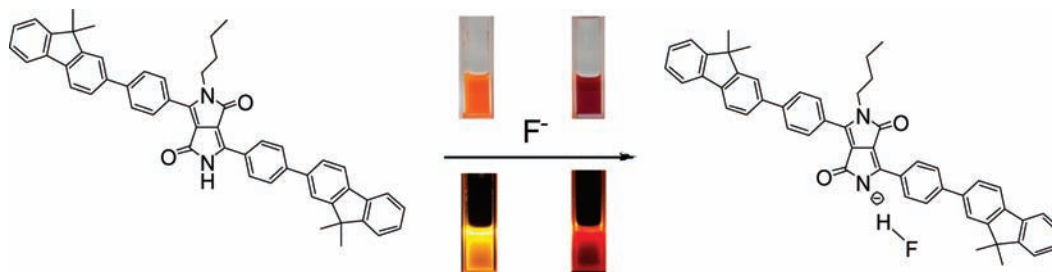
Yi Qu, Jianli Hua,* and He Tian*

Key Laboratory for Advanced Materials and Institute of Fine Chemicals, East China University of Science & Technology, Shanghai 200237, P.R. China

jlhua@ecust.edu.cn; tianhe@ecust.edu.cn

Received May 11, 2010

ABSTRACT



Three new diketopyrrolopyrrole (DPP) compounds are shown to be colorimetric and ratiometric red fluorescent sensors for fluoride anions with high sensitivity and selectivity. The recognition mechanism is attributed to the intermolecular proton transfer between a hydrogen atom on the lactam N positions of the DPP moiety and the fluoride anion.

The recognition and detection of the fluoride ion are of growing interest because it is associated with nerve gases, the analysis of drinking water, and the refinement of uranium used in nuclear weapons manufacture. As a consequence, fluoride-indicating methodologies, which are developed to provide critical information for fluoride hazard assessment and fluoride pollution management, are in high demand. Among these techniques, fluorescent molecular sensing, which translates molecular recognition into tangible fluorescence signals, has received much attention.¹ To increase the selectivity and sensitivity, ratiometric measurements are utilized, which involve the observation of changes in the ratio

of the intensities of the absorption or the emission at two wavelengths.

Ratiometric fluorescent probes have an important feature: they permit signal ratio and thus increase the dynamic range and provide built-in correction for environmental effects. The perceived color change would be useful not only for the ratiometric method of detection but also for rapid visual sensing. Up to now, many investigations have been conducted to create ratiometric fluorescent probes for cations.² In contrast, only a few ratiometric fluorescent sensors for

(1) (a) Amendola, V.; Esteban-Gómez, D.; Fabbri, L.; Licchelli, M. *Acc. Chem. Res.* **2006**, *39*, 343. (b) Esteban-Gómez, D.; Fabbri, L.; Licchelli, M. *J. Org. Chem.* **2005**, *70*, 5717. (c) Boiocchi, M.; Boci, L. D.; Esteban-Gómez, D.; Fabbri, L.; Licchelli, M.; Monzani, E. *J. Am. Chem. Soc.* **2004**, *126*, 16507. (d) Liu, Z. Q.; Shi, M.; Li, F. Y.; Fang, Q.; Chen, Z. H.; Yi, T.; Huang, C. H. *Org. Lett.* **2005**, *7*, 5481. (e) Kim, T. H.; Swager, T. M. *Angew. Chem., Int. Ed.* **2003**, *19*, 4803. (f) Uchiyama, S.; Iwai, K.; de Silva, A. P. *Angew. Chem., Int. Ed.* **2008**, *47*, 4667. (g) Nolan, E. M.; Lippard, S. J. *Chem. Rev.* **2008**, *108*, 3443. (h) Hetrick, E. M.; Schoenfish, M. H. *Annu. Rev. Anal. Chem.* **2009**, *2*, 409. (i) Zhao, Q.; Li, F. Y.; Huang, C. H. *Chem. Soc. Rev.* **2010**, DOI: 10.1039/B915340c.

(2) (a) Zhu, B. C.; Zhang, X. L.; Jia, H. Y.; Li, Y. M.; Liu, H. P.; Tan, W. H. *Org. Biomol. Chem.* **2010**, *8*, 1650. (b) Xu, Z. C.; Yoon, J. Y.; Spring, D. R. *Chem. Commun.* **2010**, *46*, 2563. (c) Ma, B. L.; Wu, S. Z.; Zeng, F. *Sensors Actuators, B* **2010**, *145*, 451. (d) Xu, Z. C.; Baek, K. H.; Kim, H. N.; Cui, J. N.; Qian, X. H.; Spring, D. R.; Shin, I. J.; Yoon, J. Y. *J. Am. Chem. Soc.* **2010**, *132*, 601. (e) Du, J. J.; Fan, J. L.; Peng, X. J.; Li, H. L.; Sun, S. G. *Sensors Actuators, B* **2010**, *144*, 337. (f) Goswami, S.; Sen, D.; Das, N. K. *Org. Lett.* **2010**, *12*, 856. (g) Wang, H. H.; Xue, L.; Qian, Y. Y.; Jiang, H. *Org. Lett.* **2010**, *12*, 292. (h) Zhou, Y.; Wang, F.; Kim, Y.; Kim, S.-J.; Yoon, J. Y. *Org. Lett.* **2009**, *11*, 4442. (i) Tian, M. Q.; Ihmels, H. *Chem. Commun.* **2009**, *45*, 3175. (j) Li, H. B.; Yan, H. J. *J. Phys. Chem. C* **2009**, *113*, 7526.

F⁻ have been reported in the literature.³ Thus, realization of ratiometric measurements for F⁻ is still a challenge.

1,4-Diketo-3,6-diphenylpyrrolo[3,4-c]pyrrole (DPP) and its derivatives represent a class of brilliant red and strongly fluorescent high performance pigments that have exceptional light, weather, and heat stability.⁴ Recently, significant progress has been made to use DPP-containing materials in polymer solar cells (PSCs),⁵ field effect transistors (FET),⁶ OLEDs,⁷ two-photon absorption,⁸ and dye sensitizing solar cell applications. Also, the hydrogen atom on the lactam N positions of the DPP moiety may be a useful receptor for fluorescence sensors, and the strong H–F interaction will result in deprotonation of a DPP amide moiety in the presence of a fluoride ion, causing a dramatic change in color and fluorescence of the compounds. In addition, a number of fluorene-based DPP compounds show good optical and electrical properties due to their high photoluminescence efficiency and good chemical and thermal stability.⁹ Therefore, it could be expected that some core-monomonsubstituted DPP derivatives with good solubility should be “naked-eye” colorimetric and ratiometric fluorescent sensors for fluoride ions. However, to the best of our knowledge, there are no reports on the fluorescent sensors based on DPP derivatives. Here, we designed and synthesized three new DPP derivatives (**1–3** shown in Figure 1), in which a long alkyl chain was contacted on the lactam N atom of the DPP moiety to improve the solubility, and some substitutes were connected to the 3,6-positions of electron-withdrawing pyrrolo[3,4-c]pyrrole-1,4-dione via 1,4-phenylene conjugation bridges, respectively. Indeed, it has been shown that even simple chromophores can operate as efficient colorimetric and ratiometric fluorescent sensors for naked-eye detection of anions.

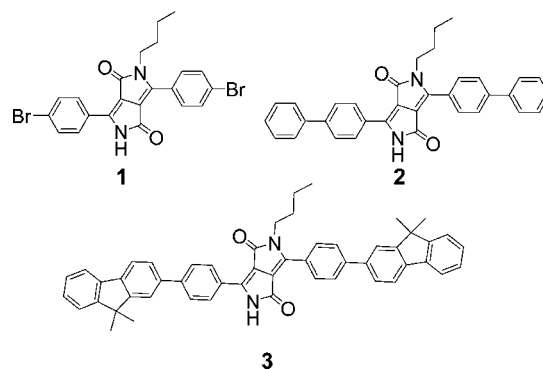


Figure 1. Molecular structures of DPP compounds **1–3**.

Synthetic routes to the DPP-based compounds (**1–3**) are shown in the Supporting Information (Scheme S1). DPP was converted to soluble DPP-R by N-alkylation of the lactam units, in which the alkyl DPP can produce the byproduct with two sides substituted; fortunately, **1** can be easily separated by column chromatography. **2** and **3** (shown in Supporting Information) were easily synthesized by the Suzuki coupling reaction **1** with phenylboronic acid and 9,9-dimethyl-9H-fluorene-2-yl boronic acid, respectively. The structures were characterized by standard spectroscopic methods (Supporting Information).

Table 1. Photophysical Properties of **1–3** in DCM^a

	$\lambda_{\text{abs}}/\text{nm}^b$	$\epsilon/10^4$	$\lambda_{\text{em}}/\text{nm}^c$
1	477	3.1	531
1F	571	1.8	613
2	485	4.4	545
2F	585	2.4	630
3	497	3.0	563
3F	594	1.6	635

^aThe photophysical properties were measured with 5.0×10^{-6} M solutions. ^bOnly the longest absorption peaks are shown. ^cEmission maximum wavelength excited at the absorbance maximum.

In the experiments, *n*-Bu₄NF (TBAF) as a fluoride source was gradually added to a dichloromethane (DCM) solution of the DPP compound. The deprotonated abilities of **1–3** with the fluoride ion were investigated by the UV–vis absorption and fluorescence spectra. Here, **1F**, **2F**, and **3F** represent the corresponding DPP-based compounds of **1**, **2**, and **3** with addition of the fluoride ion, respectively. Their photophysical properties are summarized in Table 1. When TBAF was added to the DCM solution of **3**, an apparent color change from orange to purple in ambient light, as shown in the inset of Figure 2a, can be observed by the naked eye. Upon progressive addition of TBAF, the intensity at 497 nm was gradually decreased, and a large bathochromic shift (~80 nm) of the maximum could be observed (Figure 2a). Meanwhile, a completely new band at 594 nm is developed with clear isosbestic points at 543 nm indicating

(3) (a) Liu, B.; Tian, H. *J. Mater. Chem.* **2005**, *15*, 2681. (b) Qu, Y.; Hua, J. L.; Jiang, Y. H.; Tian, H. *J. Polym. Sci., Part A: Polym. Chem.* **2009**, *47*, 1544. (c) Li, Y.; Cao, L. F.; Tian, H. *J. Org. Chem.* **2006**, *71*, 8279. (d) Mashraqui, S. H.; Betkar, R.; Chandiramani, M.; Quinonero, D.; Frontera, A. *Tetrahedron Lett.* **2010**, *51*, 596. (e) Yang, X. F.; Qi, H. P.; Wang, L. P.; Su, Z.; Wang, G. *Talanta* **2009**, *80*, 92.

(4) (a) Toyo Ink Mfg. K.K. Japan Patent. 2055-362-A, 1990. (b) Fujii Photo Film K.K. Japan Patent. 2039-159-A 1990. (c) Dainippon Ink Chem. K. K. Japan Patent. 3011-357-A, 1990. (d) Ciba-Geigy Ltd. European Patent. 0.353184-A, 1990. (e) Mizuguchi, J.; Rochat, A. C. *J. Imag. Technol.* **1991**, *17*, 123. (f) Mizuguchi, J.; Giller, G.; Baeriswyl, E. *J. Appl. Phys.* **1994**, *75*, 514. (g) LanghalsH. German Patent 3901 988, 1990. (h) Hao, Z.; Iqbal, A. *Chem. Soc. Rev.* **1997**, *26*, 203.

(5) (a) Thompson, B. C.; Fréchet, J.M. *J. Angew. Chem., Int. Ed.* **2008**, *47*, 58. (b) Wienk, M. M.; Turbiez, M.; Gilot, J.; Janssen, R. A. *J. Adv. Mater.* **2008**, *20*, 2556. (c) Tamayo, A. B.; Walker, B.; Nguyen, T.-Q. *J. Phys. Chem. C* **2008**, *112*, 11545. (d) Tamayo, A. B.; Dang, X.-D.; Walker, B.; Seo, J.; Kent, T.; Nguyen, T.-Q. *Appl. Phys. Lett.* **2009**, *94*, 103301. (e) Zhang, G. Q.; Liu, K.; Fan, H. J.; Li, Y.; Zhan, X. W.; Li, Y. F.; Yang, M. *J. Synth. Met.* **2009**, *159*, 1991.

(6) Yanagisawa, H.; Mizuguchi, J.; Aramakil, S.; Sakai, Y. *Jpn. J. Appl. Phys.* **2008**, *47/6*, 4728.

(7) Zhu, Y.; Rabindranath, A. R.; Beyerlein, T.; Tieke, B. *Macromolecules* **2007**, *40*, 6981.

(8) (a) Jiang, Y. H.; Wang, Y. C.; Hua, J. L.; Qian, S. Q.; Tian, H. *J. Polym. Sci., Part A* **2009**, *47*, 4400. (b) Guo, E. Q.; Ren, P. H.; Zhang, Y. L.; Zhang, H. C.; Yang, W. *J. Chem. Commun.* **2009**, *45*, 5859.

(9) (a) Morales, A. R.; Yanez, C. O.; Schafer-Hales, K. J.; Marcus, A. I.; Belfield, K. D. *Bioconjugate Chem.* **2009**, *20*, 1992. (b) Hung, Y.-C.; Jiang, J.-C.; Chao, C.-Y.; Su, W.-F.; Lin, S.-T. *J. Phys. Chem. B* **2009**, *113*, 8268. (c) Zhou, E. J.; Cong, J. Z.; Yamakawa, S.; Wei, Q. S.; Nakamura, M.; Tajima, K.; Yang, C. H.; Hashimoto, K. *Macromolecules* **2010**, *43*, 2873. (d) Baheti, A.; Tyagi, P.; Thomas, K. R. J.; Hsu, Y.-C.; Lin, J. T. *J. Phys. Chem. C* **2009**, *113*, 8541.

the formation of a second species with stronger push–pull electron effect. As shown in the inset of Figure 2b, the emission spectra of **3** also displayed obvious changes when the fluoride ion was added. With the fluoride ion addition, a decrease of the emission at 563 nm and the emergence of a red-shifted emission band at 635 nm were observed.

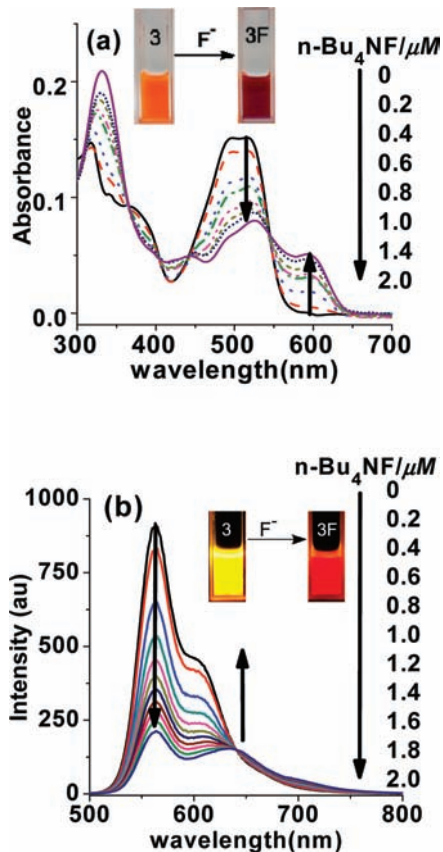


Figure 2. (a) UV–vis absorption spectra of **3** (5.0×10^{-6} M) in DCM upon addition of 0–2.0 μM of TBAF. Inset: color changes upon addition of F^- . (b) Emission spectra of **3** (5.0×10^{-6} M) in DCM upon the addition of 0–2.0 μM of TBAF. Inset: red emission during titration experiment with F^- .

On the basis of the above facts, a possible explanation for the ratiometric absorption changes is the intermolecular proton transfer (IPT) process between the amide moiety and fluoride ion and its change from electronically neutral (Ar-DPP-NH-Ar) without a fluoride ion to negatively charged (Ar-DPP-N[−]-Ar) with a fluoride ion (Scheme 1). The modulation in the electron-donating capabilities of the amide group in the presence and absence of fluoride directly influences the internal charge transfer (ICT) from the amide moiety to the conjugated system of the sensors. In the presence of fluoride, the ICT effect from the amide anion to the electron-withdrawing moiety is enhanced, which was facilitated by the deprotonation of the amide moiety. This enhancement in ICT effect also affords the reduced intensity and bathochromic shift of fluorescence as a function of fluoride concentration.

Scheme 1. Intermolecular Proton Transfer between **3** and the Fluoride Ion

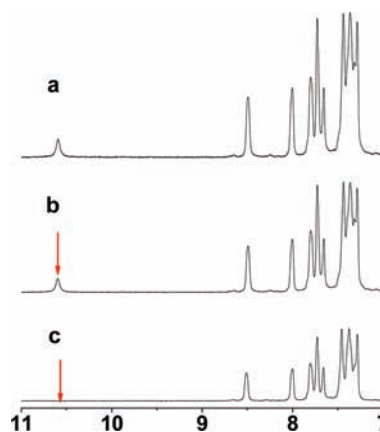
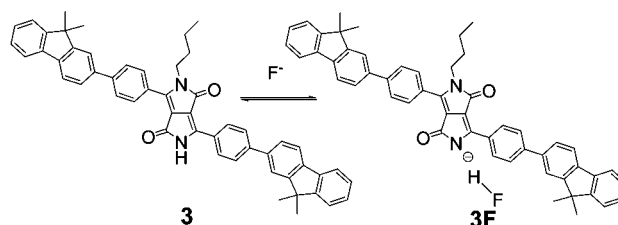


Figure 3. Partial ^1H NMR spectra of sensor **3** in CDCl_3 in the presence of (a) 0 equiv, (b) 1 equiv, and (c) 2 equiv of TBAF.

To confirm this assumption, proton NMR titrations were carried out (Figure 3). It was found that the amide NH proton signal (~ 10.56 ppm) decreased and finally disappeared with addition of F^- , which is well recognized to be due to hydrogen bonding formation; therefore, the result is consistent with the breaking of hydrogen bonding when the fluoride ion was added.

A near-linear correlation of sensor **3** between intensity ratios of absorbance at 594 nm to those at 497 nm (A_{594}/A_{497}) vs fluoride ion concentration in DCM was obtained (Figure 4a).

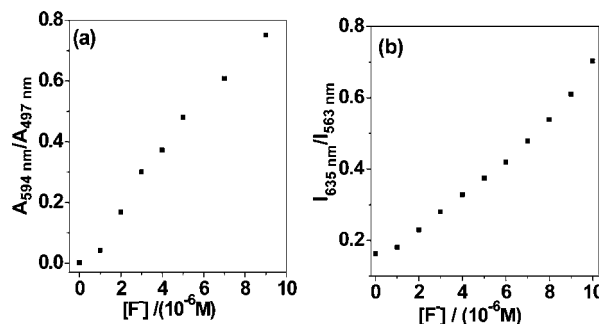


Figure 4. (a) Plot of the absorbance ratio of **3** between 594 and 497 nm ($A_{594\text{ nm}}/A_{497\text{ nm}}$) vs concentration of F^- in DCM. (b) Plot of the emission intensity ratio of **3** between 635 and 563 nm ($I_{635\text{ nm}}/I_{563\text{ nm}}$) vs concentration of F^- in DCM.

This demonstrates the potential utility of sensor **3** for calibrating and determining fluoride ion concentration in DCM. Furthermore, F^- could be detected at the parts per million level when sensor **3** was employed at 5.0×10^{-6} M, and A_{594}/A_{497} also increased linearly in this concentration range. A corresponding correlation between emission ratiometric response of **3** at 635 and 563 nm (I_{635}/I_{563}) and fluoride ion concentration in DCM was obtained in Figure 4b which demonstrated that **3** can serve as a ratiometric fluorescent sensor for F^- . Similar effects were observed for **1** and **2** (see Supporting Information).

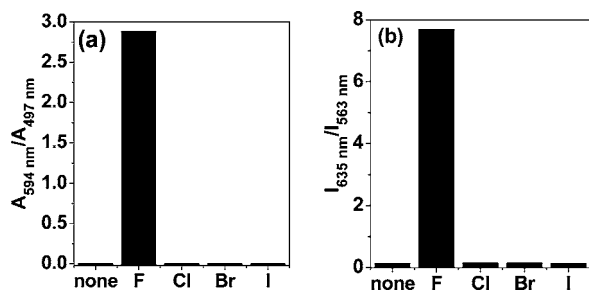


Figure 5. (a) Absorbance ratiometric response of **3** between 594 and 497 nm to the halide ions (150 μ M). (b) Emission ratiometric response of sensor **3** to the halide ions (150 μ M). The emissions were at 635 and 563 nm and excited at 435 nm.

The experimental results suggest that compound **3** shows high selectivity in colorimetric and fluorescent sensors for the fluoride anion. As depicted in Figure 5a, the absorbance at 594 nm was approximated 3-fold than that at 497 nm with addition of 30 equiv of TBAF. Furthermore, no changes were found with addition of other halide ions (also see Figure S6 in the Supporting Information). Figure 5b shows that emission intensity at 635 nm of **3** was approximated 8-fold than that at 563 nm with addition of 30 equiv of F^- , while Cl^- , Br^- , and I^- caused no changes in the emission spectra. Moreover, the selective properties of **1** and **2** show a similar response to the titration of TBAF (Figure 6). Appearance of the red color and red emission of **1** and **2** can also be expected because of deprotonation of the NH proton caused by TBAF addition. However, other halide ions produced insignificant changes in both absorption and emission spectra.

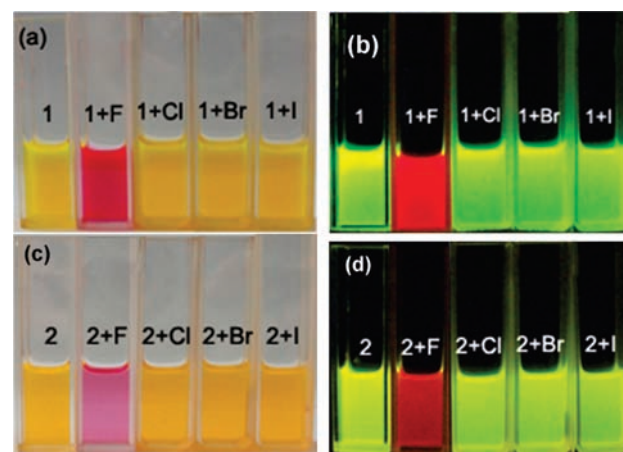


Figure 6. (Top) Color (a, left) and fluorescence (b, right) change of **1** (from left to right: **1** only; **1** + F^- ; **1** + Cl^- ; **1** + Br^- ; **1** + I^-). (Bottom) Color (c, left) and fluorescence (d, right) change of **2** (from left to right: **2** only; **2** + F^- ; **2** + Cl^- ; **2** + Br^- ; **2** + I^-).

In summary, we have developed a novel prototype of highly efficient colorimetric and fluorescent fluoride sensors **1–3** incorporating DPP. For receptors **1–3** in DCM, the addition of fluoride results in *vivid* orange-to-red absorption color change and yellow-to-red emission color change due to deprotonation, in which **3** exhibits the best sensitive property and detects fluoride concentrations in a range of 0–10 μ M at visible region wavelengths. The core mono-substituted DPP design is an effective approach to develop novel colorimetric and red fluorescent fluoride sensors.

Acknowledgment. This work was supported by NSFC/China (20772031), National Basic Research 973 Program (2006CB806200), the Fundamental Research Funds for the Central Universities (WJ0913001), and the Scientific Committee of Shanghai.

Supporting Information Available: Synthetic procedures of sensors **1–3**, the absorption and fluorescent titration study of sensors **1** and **2**, full characterization for the DPP sensors (**1–3**) described in this paper, and the pictures of the sensors with addition of different halide ions. This material is available free of charge via the Internet at <http://pubs.acs.org>.

OL101081M